

Materials and Mechanisms of Photo-Assisted Chemical Reactions under Light and Dark Conditions: Can Day–Night Photocatalysis Be Achieved?

M. Sakar, Chinh-Chien Nguyen, Manh-Hiep Vu, and Trong-On Do*^[a]

The photoassisted catalytic reaction, conventionally known as photocatalysis, is expanding into the field of energy and environmental applications. It is widely known that the discovery of TiO₂-assisted photochemical reactions has led to several unique applications, such as degradation of pollutants in water and air, hydrogen production through water splitting, fuel conversion, cancer treatment, antibacterial activity, self-cleaning glasses, and concrete. These multifaceted applications of this phenomenon can be enriched and expanded further if this process is equipped with more tools and functions. The term “photoassisted” catalytic reactions clearly emphasizes that pho-

tons are required to activate the catalyst; this can be transcended even into the dark if electrons are stored in the material for the later use to continue the catalytic reactions in the absence of light. This can be achieved by equipping the photocatalyst with an electron-storage material to overcome current limitations in photoassisted catalytic reactions. In this context, this article sheds lights on the materials and mechanisms of photocatalytic reactions under light and dark conditions. The manifestation of such systems could be an unparalleled technology in the near future that could influence all spheres of the catalytic sciences.

1. Introduction


Research into energy and environmental concerns has increased in recent years more than ever before.^[1,2] Of various strategies to address these concerns, photoassisted catalytic processes play vital roles.^[3–5] It is not an exaggeration to state that photoassisted chemical reactions are a promising phenomenon that could be employed for several applications, such as environmental cleaning through degradation of various pollutants, production of hydrogen through the water-splitting process, and fuel conversion.^[6–8] In this context, materials are the key factors to manifest the required phenomenon to successfully achieve the target applications. In brief, the phenomenon of photoassisted chemical reactions involves the absorption of light and the separation of excitons to produce potential redox species to perform the reduction and oxidation reactions.^[9] For this to happen effectively, the photoactive materials require 1) a suitable band edge position, 2) a narrow band gap energy, 3) improved charge separation and transportation, 4) enhanced recombination resistance, and 5) effective interfacial interactions.^[10–12]

Among these criteria, the prime focus has been on the development of materials with tunable band gap energies and band edge positions in such a way to produce the required redox species and, essentially, to absorb full-sunlight energy, which is the UV/Vis/near-IR (NIR) range of the solar spectrum.^[13] Although the established photocatalytic material TiO₂

is UV-light driven, the emergence of visible/full-sunlight-driven photocatalytic materials in recent years is gaining momentum in their design and development for photocatalytic applications.^[14–16] The quest to explore such materials is to utilize the earth-abundant light energy source, sunlight. Moreover, the industrial-scale development of such a light source is also a straightforward strategy to perform photocatalytic reactions in controlled and portable environments. Notably, solar energy that falls upon the earth consists of 5, 45, and 50% UV, visible, and NIR energies, respectively.^[17] In the photocatalytic process, the band edge positions of the valence band (VB) and conduction band (CB) are of foremost importance in designing a photocatalyst (PC). Figure 1 shows various redox conversions and their respective potential on the scale of a normal hydrogen electrode (NHE).^[18] The most challenging and interesting factor in designing a full-sunlight-driven PC is to control both the band edge position and band gap energy.^[19] However, these two factors overlap with each other and are mutually exclusive in achieving a PC with a tunable band edge position and narrow band gap energy. Nevertheless, this can still be achieved by the appropriate fusion of materials with specific characteristics of harvesting UV, visible, and NIR energies.^[20]

However, currently there is a paradigm shift in the field towards developing photocatalytic materials to perform photocatalytic reactions under both light and dark conditions, which is “day–night” photocatalysis, otherwise known as “round-the-clock photocatalytic reactions”, as evidenced from the literature discussed herein. Apart from the fundamental requirements for photocatalysis, there is one more component, which is known as the electron-storage material (ESM), primarily required to allow a PC to catalyze a reaction under dark condi-

[a] Dr. M. Sakar, C.-C. Nguyen, M.-H. Vu, Prof. T.-O. Do
Department of Chemical Engineering, Laval University
Québec G1V 0A6 (Canada)
E-mail: trong-on.do@gch.ulaval.ca

 The ORCID identification number(s) for the author(s) of this article can be found under <https://doi.org/10.1002/cssc.201702238>.

Sakar Mohan is a postdoctoral research fellow under the supervision of Prof. Trong-On Do in the Department of Chemical Engineering, Laval University, Canada. He obtained his M.Sc., M.Tech, and PhD degrees in 2010 and 2015, respectively, from the University of Madras, India. His research focuses on the development of photocatalytic nanomaterials for energy and environmental applications. Currently, he has published over 30 research articles in refereed international journals.



Chinh-Chien Nguyen obtained his BSc and MSc degrees from the Chemistry Department of the Hue University of Sciences, Vietnam, in 2009 and 2011, respectively. He is currently working for his PhD degree at Laval University, Canada, under the supervision of Prof. Trong-On Do. His research focuses on the development of novel photocatalysts for water splitting and pollutant degradation through solar energy.



Manh-Hiep Vu obtained his BSc from the Chemistry Department of the Vietnam National University in 2014. He is currently working for his PhD degree at Laval University, Canada, under the supervision of Prof. Trong-On Do. His research focuses on the development of novel photocatalysts for water splitting and nitrogen photofixation through solar energy.



Trong-On Do is a full professor in the Department of Chemical Engineering at Laval University, Canada. He received his MSc and PhD from University of P. and M. Curie (France) and carried out postdoctoral research in Prof. G. Bond's group at Brunel University (UK) and French Catalysis Institute (France). He spent two years (1997–1999) in the Hashimoto/Fujishima group at KAST under the Japanese STA Fellowship Award. His current research focuses on the design and synthesis of innovative and smart nanomaterials as photocatalysts and their applications in renewable energy and environmental remediation. He has published over 140 research articles and is the recipient of the 2015/2014 Canadian Catalysis Lectureship Award.



tions.^[21] The mechanism of the ESM involves the storage of electrons by forming an intermediate compound during the catalytic reactions under light irradiation, and reverting to release the electrons in the absence of light. Briefly, under light irradiation, electrons are photoexcited from the VB to the CB and involved in photocatalytic reactions, whereas excess electrons are stored in the ESM. These stored electrons continue the photocatalytic activity through cathodic reactions in the absence of light. Thus, the ESM is photocharged under light irradiation and auto-discharged in the absence of light. It should be noted that in these processes only electrons are involved in the reactions and the holes in the VB are mostly promoted to the surface of the PC and perform some oxidation reactions, such as the oxidation of water. Therefore, day–night photocatalysis can be achieved by combining 1) a PC and 2) an ESM. In this context, herein, we provide a perspective on the materials and mechanisms of the day–night PC and its photocatalysis phenomenon.

2. Components and Mechanism of the Day–Night PC

As aforementioned, a day–night photocatalytic system is generally composed of two kinds of materials: 1) any typical PC and 2) an ESM. The PC will harvest energy by absorbing light, as dictated by its band gap energy, and promotes charge carriers for photocatalytic reactions. Among the number of electrons excited, electrons with the potential of performing reduction reactions are involved in the photocatalytic activity, whereas the excess electrons are transferred to the ESM for later use. On the other hand, separated holes in the VB perform surface reactions. The storage of electrons is possible because of the intermediate cationic formation of the ESM or the host PC itself (in some cases), which is essentially a charge–discharge-like reaction. The storage of electrons occurs if the process of electron excitation is ON under light irradiation. As soon as light irradiation or the charging process is stopped, the reaction becomes opposite and discharges stored electrons, so that they are involved in photocatalytic processes. Accordingly, there are typically three kinds of electron-storage mechanisms perceived in the day–night photocatalytic process, of which the mechanism that is occurring depends upon the types of materials involved.

2.1. Reductive mechanism

Materials such as TiO₂–WO₃ store electrons through reductive reactions,^[21,22] with the formation of an intermediate reversible product, as described in Equations (1)–(3), in which TiO₂ functions as a PC and WO₃ as an ESM.



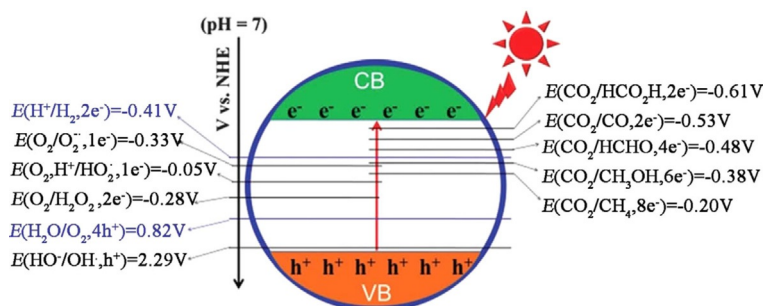


Figure 1. Redox conversions of different species and their respective potentials.

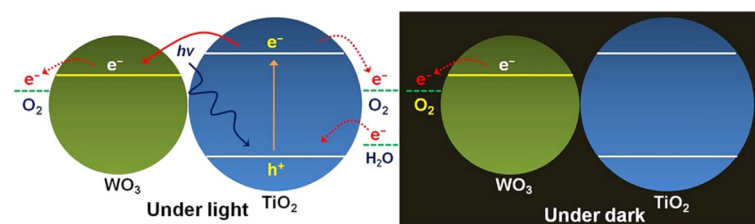


Figure 2. Reduction mechanism mediated electron storage in the TiO_2 - WO_3 system.

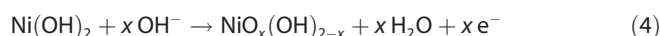
As the system is irradiated with light, electrons and holes are photogenerated [Eq. (1)]. Furthermore, holes are promoted to the surface of TiO_2 , where they react with adsorbed H_2O /humid air or other electrolytes and produce O_2 and H^+ (in the case of H_2O) or M^+ (in the case of other electrolytes; M can be Li, Na, K, Rb, Ca, Sr, Ba, Al, In, Tl, Sn, Pb, Cu, Ag, Cd, rare-earth elements, or NH_4^+),^[23] as given in Equation (2). On the other hand, available photoinduced electrons facilitate the intercalation of H^+ or M^+ ions into WO_3 , through which a chemically reversible intermediate compound is formed [Eq. (3)]. H^+ is the only available cation in pure water, but it can also be M^+ if an electrolyte is used instead. Figure 2 depicts the mechanism of reductive storage of electrons under light irradiation and release of electrons in the dark.

2.2. Oxidative mechanism

Energy can be stored in two different approaches through the oxidative mechanism: 1) the p-n junction model and 2) the mediation model.^[24] In the former, a redox-reaction-active p-type semiconductor is coupled with an n-type semiconductor to form a p-n junction. Upon excitation, holes will be transported to the p-type semiconductor for oxidative storage, in which electrical neutrality will be maintained by the intercalation of anions or deintercalation of cations; thus the oxidative energy will be maintained stably. In the second model, an oxidant is photocatalytically produced through the oxidation reaction and it oxidizes the redox-active material.

Figure 3a and b shows the energy-storage mechanism in the p-n junction and mediation models, respectively. The oxidative mechanism of energy storage has been demonstrated in the TiO_2 - $\text{Ni}(\text{OH})_2$ system. As the system is photoexcited, as given in Equation (1), the electrons are promoted to the CB of TiO_2 or at the TiO_2 - $\text{Ni}(\text{OH})_2$ junction and $\text{Ni}(\text{OH})_2$ is photocatalytically oxidized (i.e., oxidative energy is stored in $\text{Ni}(\text{OH})_2$), as given in Equation (4), and the formed intermediate ($\text{NiO}_x(\text{OH})_{2-x}$) further oxidizes the substances, as given in Equation (5). The electrons from $\text{Ni}(\text{OH})_2$ [Eq. (4)] are combined with the holes in TiO_2 . On the other hand, it is also possible that the photoexcited electrons in TiO_2 are consumed by an electron acceptor, such as active oxygen species ($^{\cdot}\text{OH}$, H_2O_2 , $\text{O}_2^{\cdot-}/\text{HO}_2^{\cdot}$) and leading to the formation of oxidative species, as given in Equations (5) and (6).

formed intermediate ($\text{NiO}_x(\text{OH})_{2-x}$) further oxidizes the substances, as given in Equation (5). The electrons from $\text{Ni}(\text{OH})_2$ [Eq. (4)] are combined with the holes in TiO_2 . On the other hand, it is also possible that the photoexcited electrons in TiO_2 are consumed by an electron acceptor, such as active oxygen species ($^{\cdot}\text{OH}$, H_2O_2 , $\text{O}_2^{\cdot-}/\text{HO}_2^{\cdot}$) and leading to the formation of oxidative species, as given in Equations (5) and (6).



Therefore, the oxidative storage that occurs as given in Equations (4) and (5) represents the p-n junction model, whereas that in Equations (6) and (7) represents the mediation model. These types of mechanisms are experimentally demon-

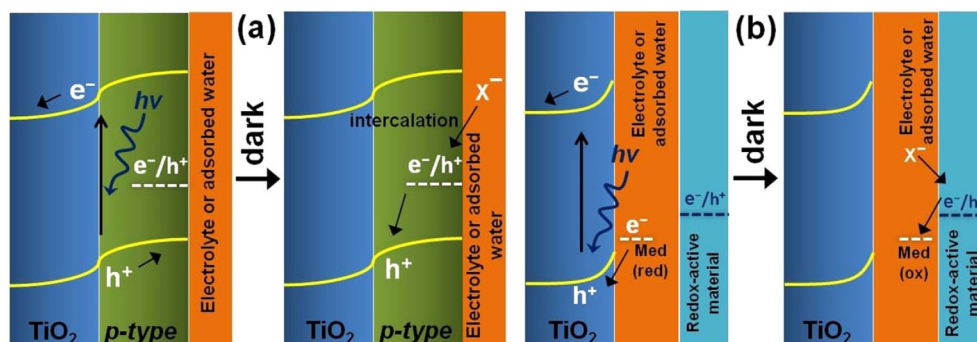


Figure 3. Oxidative energy storage through a) the p-n junction model and b) mediator model.

strated;^[24] the redox reaction at the junction is likely to determine the reaction model that takes place, namely, either oxidative storage through oxidation of the ESM or electron acceptors produced during the reaction. However, the electron-storage efficiency of this system is reportedly smaller than that of the reduction electron-storage system (TiO₂–WO₃). This is possibly due to the consumption of holes by adsorbed water oxidation or rereduction of Ni(OH)₂ by either excited electrons in TiO₂ or reductive reaction products, such as H₂O₂. Furthermore, it is also suggested that the electron-storage efficiency could be improved in the p–n junction model by increasing the junction area, such as by making the TiO₂ layers into a porous structure. Similarly, to improve the mediation model, the distance between TiO₂ and Ni(OH)₂ may be optimized to suppress the rereductive reaction by electrons in TiO₂.

2.3. Multielectron-storage mechanism

Similar to oxidative electron storage, the process of multielectron storage also occurs through two mechanisms: 1) electron reduction^[25] and 2) electron trapping.^[26] These two mechanisms of electron storage have been demonstrated in TiO₂–Cu₂O composite thin films.

According to the former mechanism, the storage of electrons occurs in TiO₂–Cu₂O thin films under visible-light irradiation through the reduction of Ti⁴⁺ ions into Ti³⁺ ions. Figure 4a shows the process of electron storage through the elec-

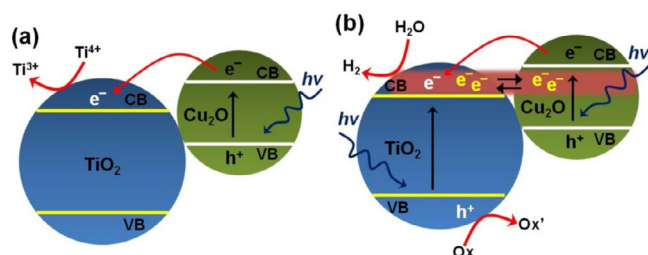


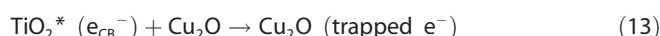
Figure 4. Multielectron-storage mechanisms through a) electron reduction and b) the electron trapping process.

tron reduction mechanism.^[25] It should be noted that the band gap energy of TiO₂ is 3.2 eV and its CB potential lies at –0.2 eV, whereas the CB potential of Cu₂O, which has a band gap energy of 2.0 eV, lies at –1.4 eV. Accordingly, it is proposed that the electrons photoinduced in the CB of Cu₂O are captured by Ti⁴⁺ ions in TiO₂ and reduced to Ti³⁺ ions, as given in Equations (8) and (9). These stored electrons are further released in the absence of light because the conversion of Ti⁴⁺ into Ti³⁺ is stopped.



In the latter mechanism,^[26] it is proposed that the electrons are captured in an electron trapping center at the TiO₂–Cu₂O junction, rather than the reduction of Ti⁴⁺ ions into Ti³⁺. This is

because, in the former mechanism, the TiO₂–Cu₂O system is excited under visible light; TiO₂ is not excited by visible light, but Cu₂O can be. Therefore, electrons excited to the CB of Cu₂O would be injected to TiO₂ and reduce Ti⁴⁺ ions into Ti³⁺. On the other hand, if the TiO₂–Cu₂O system is excited by using UV/Vis light, it is possible for the excited electrons of both TiO₂ and Cu₂O to be captured in an intermediate band, which is known as the electron trapping center, as shown in Figure 4b. The reaction process is detailed in Equations (10)–(13).



The formation of an electron trapping center essentially occurs due to the large potential difference between the CBs of TiO₂ (–0.2 eV) and Cu₂O (–1.4 eV). Hence, excess electrons in the CB of TiO₂ are facilitated to be transported to the deeply trapped state underneath the CB of Cu₂O, as shown in Figure 4b. Therefore, the essential requirement of the multielectron-storage mechanism is the combination of materials with a large difference in CB potential, which leads to a gradient band dispersion that sufficiently acts as an electron trapping center in the system.

The electron trapping process inducing photocatalytic reactions in the dark is also demonstrated in the layer-structured La₂NiO₄ (LNO) perovskite material.^[27] In this case, the LNO crystals could trap electrons from the reactant molecules (e.g., 4-chlorophenol (4-CP)) that are released in the dark for further catalytic degradation in the absence of light. Figure 5 and Equations (14)–(18) show the proposed mechanism for the degradation of 4-CP by LNO in the dark. In this mechanism, first, the ionization of 4-CP molecules into H⁺ and 4-CP[–] takes place in aqueous solution, then 4-CP[–] donates electrons to LNO (stored as trapped electrons in LNO), along with the formation of the 4-CP[•] radical. Furthermore, these trapped electrons in LNO could react with dissolved O₂ to produce [•]O₂[–], which further reacts with H⁺ and produces [•]OH radicals. Subsequently, these highly active [•]OH radicals could oxidize 4-CP[•]

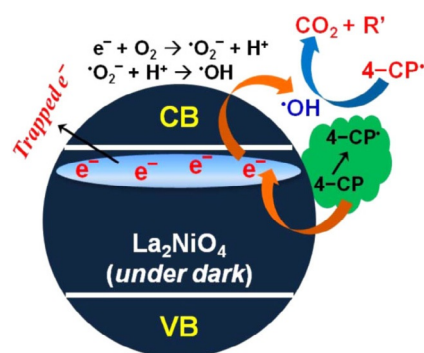
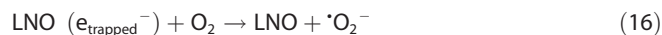
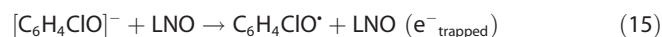


Figure 5. Degradation mechanism of 4-CP by LNO PC in the dark.

radicals and degrade into CO_2 and other products [Eqs. (14)–(18)]. It is further highlighted that the ability of LNO to trap electrons from the reactant molecules determines its degradation efficiency in the dark.



3. Prospective Materials

The first working electron-storage system, $\text{TiO}_2\text{--WO}_3$, was developed by Fujishima et al. for anticorrosion applications under light and dark conditions.^[22] The concept of photoelectrochemical anticorrosion with the energy-storage ability of the system is depicted in Figure 6.

If the system is excited by an appropriate light source, electrons in the VB are excited to the CB and these excited electrons are injected into the metal. This essentially keeps the potential more negative than that of the corrosion potential. Excess electrons are taken up by the ESM, and thus, the reductive energy produced at the excited semiconductor can be stored. After turning off the light, the stored electrons in the ESM are injected into the metal; thus it is being continuously protected from corrosion. Later, the same group demonstrated the ability of the $\text{TiO}_2\text{--WO}_3$ composite PC to store energy if pure water and air are used as the background instead of an electrolyte. Based on this work, it was proposed that energy-storage PCs could also be used for bactericidal applications and eventually it was also demonstrated by the same

group in 2003.^[28] As a further development in this system, $\text{TiO}_2\text{--WO}_3$ was combined with other ESMs, such as phosphotungstic acid^[29] and MoO_3 .^[30]

As discussed in Section 2, oxidative energy storage was first observed in the $\text{TiO}_2\text{--Ni(OH)}_2$ PC in 2005,^[24] with an expectation that the combination of reduction and oxidative energy-storage types would enhance the effective storage of energy and its later usage. Then, based on the concept of plasmon sensitization of the PC, the Au--TiO_2 system was developed and coupled with WO_3 and MoO_3 materials and studied for their energy-storage abilities under visible-light irradiation, as depicted in Figure 7.^[31]

Interestingly, the process of energy storage and later utilization was termed the “photocatalytic memory” effect, as coined by Shang et al. in 2008.^[32] They developed palladium oxide nanoparticles dispersed in nitrogen-doped TiO_2 (TiON/PdO) fibers and studied their photocatalytic disinfection properties on *Escherichia coli*, for which they observed a remarkable photocatalytic memory induced disinfection capability of the material in the absence of light, which was extended up to 8 h. Notably, the system composed of $\text{TiO}_2\text{--V}_2\text{O}_5$ was further developed and investigated for its photocharging and discharging abilities towards the photocatalytic oxidation of methanol.^[33]

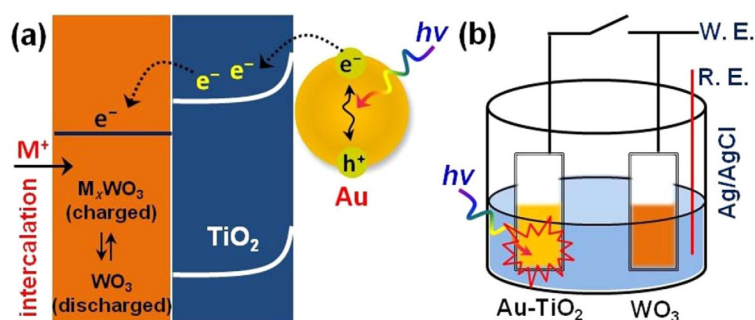


Figure 7. a) Electron-storage process in the $\text{Au--TiO}_2/\text{WO}_3$ system and b) the experimental setup. W.E. = working electrode, R.E. = reference electrode.

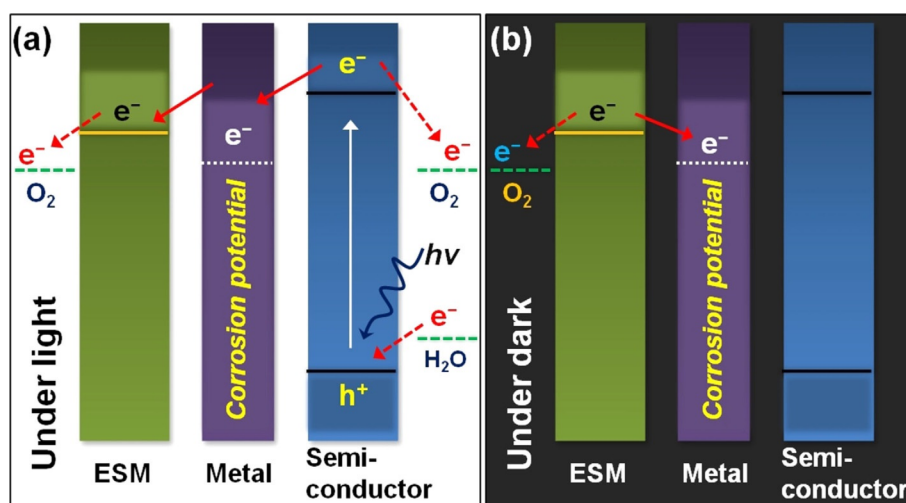
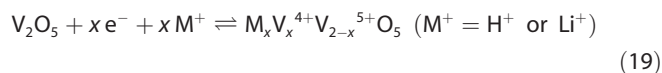


Figure 6. Mechanism of the anticorrosion process in the metal coupled with an energy storage system (semiconductor) under light irradiation (a) and dark (b) conditions.

The energy-storage mechanism in this system was proposed to be that electrons could accumulate in the V_2O_5 matrix through the intercalation of H^+ or Li^+ ions to form a bronze structure of V_2O_5 , as shown in Equation (19). It is also proposed that V_2O_5 facilitates energy storage due to the relative CB potentials of the V_2O_5 - TiO_2 system and both the V^{4+}/V^{5+} redox pair and shcherbinaite structure are responsible for the trapping of photoelectrons in V_2O_5 .



Significant results from the photoinduced electron-storage mechanisms further led to the development of new and modified systems, such as TiO_2 - N_x /NiO bilayer thin films,^[34] WO_3 ,^[35] TiO_2 -SWCNT (SWCNT = single-walled carbon nanotubes),^[36] Ag - TiO_2 ,^[37] Pt - WO_3 , Cu^{II} - WO_3 ,^[38] $Ni(OH)_2$ -coupled N-doped TiO_2 , Fe^{II} - TiO_2 , Cu^{II} - WO_3 , Pt - WO_3 ,^[39] hydrogen-treated Pt - WO_3 ,^[40] Cu_2O/TiO_2 ,^[41] Ag - In - Ni - S nanocomposites,^[42] H : Pt - WO_3/TiO_2 - Au nanospheres,^[43] $TiO_2/SiO_2/MnO_x$,^[44] SnO_2 -decorated Cu_2O ,^[45] TiO_2 - NiO/TiO_2 film,^[46] graphitic carbon nitride (g - C_3N_4)/carbon nanotubes (CNTs)/graphene (Gr),^[47] modified carbon nitride,^[48] Au - ZnO ,^[49] Pt -loaded $TiO_2/CeO_2/SiO_2$,^[50] Ag - ZnO ,^[51] N - TiO_2 ,^[52] metal-organic frameworks on Au/TiO_2 ,^[53] nickel sulfide,^[54] Ag -modified PCs,^[55] ZnO_2 /polypyrrole,^[56] and Rh/Au -modified Al_2O_3 ,^[57] and studied for their day-night photocatalytic properties, as discussed in the following sections.

A round-the-clock photocatalytic process is another description of the catalytic functionality of a PC under light and dark conditions. This can be achieved either by coating a phosphorescence material in the photocatalytic reaction chamber^[58-60] or by compositing it with the PC.^[61] The phosphorous material serves as a light source if the external light source is stopped or not available, as illustrated in Figure 8.^[61] As a result, the PC in the vicinity of the phosphorous material performs photocatalytic reactions round the clock. The concept of "dark" in the round-the-clock process is the unavailability of external light sources, such as simulated solar light or UV light. However, the PC will be irradiated with the phosphor material in the dark. The long-afterglow phosphor is a functional phosphor material that shows several hours of phosphorescence. It has been reported that the silicate-based phosphor SMSO is a potential blue-light-emitting long-afterglow phosphor that can excite

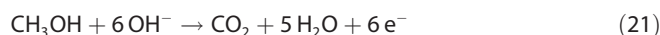
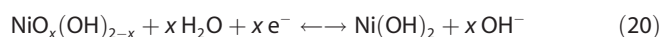
the g - C_3N_4 PC.^[62,63] Accordingly, Zhou et al. reported the photocatalytic degradation of rhodamine B and methyl orange (MO) by using SMSO/ g - C_3N_4 composite PC, which showed degradation activity for 6 h in the absence of an external light source.^[61]

4. Applications of the Day-Night Photocatalytic Systems

The exploration of energy-storage materials for day-night photocatalysis has increased in recent years; this is mainly inspired by the TiO_2 - WO_3 system for its anticorrosion effect under dark conditions. However, because TiO_2 - WO_3 is fundamentally a photocatalytic system, the subsequent development of such energy-storage materials is largely directed towards their photocatalytic applications, such as hydrogen production, pollutant degradation, heavy-metal reduction, bactericidal disinfection, and other photocatalytic applications under light irradiation and dark conditions.

4.1. Pollutant degradations

TiO_2 - $Ni(OH)_2$ was the first system studied for its day-night photocatalytic degradation applications.^[64] This bilayer photocatalytic system was investigated exclusively for its oxidatively stored energy to degrade methanol and formaldehyde under UV-light irradiation. It was reported that, if the concentration of methanol in air was as low as 10 ppm, the effective mass conversion from methanol to CO_2 was around 86% in the dark. The authors also concluded the formaldehyde could also be oxidized to CO_2 by the stored energy. They proposed the mechanism in Equations (20)–(22) for the degradation of methanol and formaldehyde by the oxidative storage energy of the TiO_2 - $Ni(OH)_2$ PC.



The dark photocatalytic properties of the WO_3/TiO_2 system were studied for the degradation of MO dye.^[65] Initially, the WO_3/TiO_2 PC was irradiated under visible light for 40 min.

Then, the dye molecules were added to the solution of PC after the light was turned off. After 40 min under dark conditions, 22% of MO dye was degraded. It was also found that increasing concentrations of WO_3 increased the degradation efficiency of this photocatalytic system. Furthermore, it was also reported that the agitation effect during dark catalysis had no influence on the degradation efficiency of the day-night PC.

In another report, bare and hydrogen-treated platinum-loaded WO_3 systems (Pt - WO_3 and Pt - H : WO_3 , respectively) were studied for their ability to degrade formaldehyde under irradiation and dark conditions.^[40] The degradation of formaldehyde into CO_2

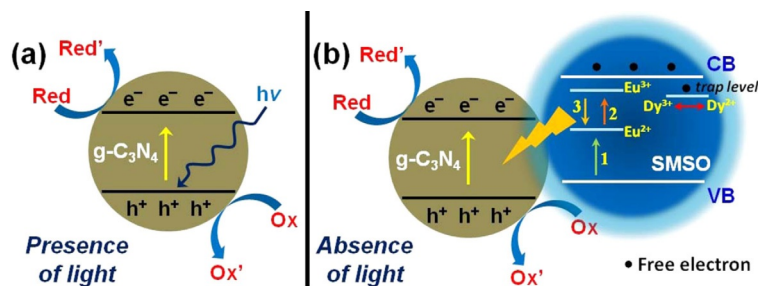


Figure 8. a)–b) Illustration of the round-the-clock photocatalytic mechanism assisted by long-afterglow phosphorescence in the $Sr_2MgSi_2O_7:(Eu, Dy)$ (SMSO)/ g - C_3N_4 PC in the presence (a) and absence (b) of light.

by Pt–WO₃ and Pt–H:WO₃ was observed under visible-light irradiation for 60 min. Subsequently, the light was turned off after 60 min and the degradation of formaldehyde was continuously observed for up to 360 min in the dark. Interestingly, the stability of the stored energy was also tested, for which the sample was kept in the dark for 12 h and eventually it was observed that Pt–WO₃ and Pt–H:WO₃ degraded around 20 and 80% of formaldehyde, respectively, after 360 min in the dark. Furthermore, the degradation of gaseous-phase formaldehyde by Pt–H:WO₃ was also studied, for which the sample was photocharged for 1 h and stored in the dark for up to 300 h. After 36, 276, and 300 h, the degradation ability was recorded over a period of 6 h in the dark. At the end of 300 h, the dark degradation was estimated to be 60%. To further evaluate long-lasting usage, the recovered Pt–H:WO₃ PC was again irradiated for 1 h and the catalytic activity was observed over a period of 6 h in the dark. The catalytic effect of Pt–H:WO₃ in the dark was persistently observed, even after the PC was heated at 200 °C for 2 h. The mechanism of the observed long, persistent, catalytic properties of Pt–H:WO₃ in the dark is depicted in Figure 9 and proposed to occur as follows: 1) Hydrogen treat-

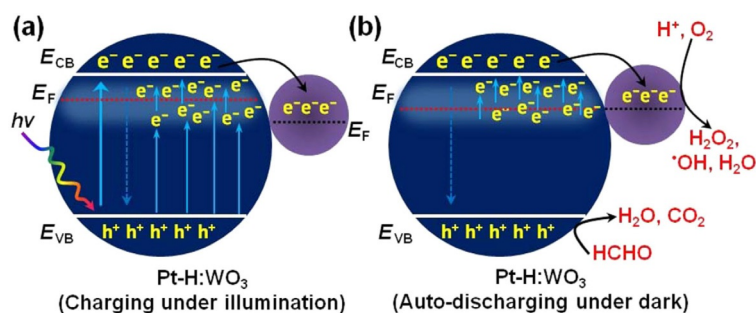


Figure 9. Mechanism of photoelectron storage under illumination (a) and release of electrons in the dark (b) for the Pt–H:WO₃ system.

ment led to the formation of large amounts of oxygen vacancies in WO₃, and induced defect band structures in its band gap structure. These defect bands caused an upshift in the Fermi level and provided more trapping sites to store electrons for a superlong time. 2) Loaded Pt nanoparticles enhanced formaldehyde degradation by facilitating multielectron reduction of O₂ on Pt.

The Cu₂O/TiO₂ composites, consisting of TiO₂ islands decorated with Cu₂O nanospheres, were prepared and investigated for the degradation of MO under visible-light irradiation and dark conditions.^[41]

It was reported that the residual percentage of MO was about 3 and 80% under visible-light irradiation and dark conditions, respectively. The mechanism of the observed activity was attributed to the difference in band potential and electrostatic field at the interface of Cu₂O and TiO₂, at which it facilitated the transfer of excess electrons from the CB of Cu₂O to TiO₂ and stored trapped electrons by reducing Ti⁴⁺ into Ti³⁺ for later release in the dark, as shown in Figure 10. These stored electrons react with O₂ to produce superoxide radicals

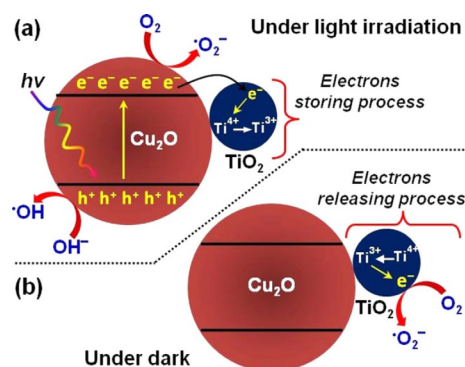


Figure 10. Reduction-mediated electron storage and release in the Cu₂O/TiO₂ photocatalytic system in the presence (a) and absence (b) of light.

and the holes in Cu₂O react with water to produce hydroxyl radicals to degrade the dye in the dark.

Interestingly, an unconventional material, Ag–In–Ni–S nanocomposite, was proposed for the photocatalytic degradation of methylene blue (MB) dye molecules under visible-light and dark conditions.^[42] In this study, the photocatalytic activity of the prepared material was investigated in the absence and presence of visible light (sunlight and 100 W tungsten lamp). Notably, this material showed complete degradation of a given amount of dye under lamp and sunlight in 4 and 2 min, respectively, whereas it took 12 min for complete degradation of the dye under dark conditions. It is proposed that, in the Ag–In–Ni–S nanocomposite, the electron-storage properties of silver help to shift the Fermi level of the composites toward more negative values that make the PC more reductive. This reductive nature of the PC tends to supply electrons, even under dark conditions, and leads to the production of redox species. It was also proposed that the cascading band structure between the integrated materials could also have facilitated the transfer and storage of electrons under irradiation and their release under dark conditions.

In our group, we have developed the hollow double-shell H:Pt–WO₃/TiO₂–Au nanospheres and studied their photocatalytic activity on the conversion of formaldehyde (HCHO) into CO₂ under visible-light irradiation and dark conditions.^[43] At the end of 6 and 16 h, more than 90 and 80% of HCHO was converted into CO₂ under visible-light and dark conditions, respectively. Similarly, other systems, such as hollow H:Pt–WO₃/TiO₂ and hollow H:Pt–WO₃, showed 42 and 36% HCHO conversion, respectively, at the end of 6 h under visible light, whereas they showed 39 and 40% conversion, respectively, after 18 h under dark conditions. The observed results were attributed to the presence of a large amount of oxygen vacancies in WO_{3–x}, which facilitated the trapping of electrons under light irradiation and release of the electrons under dark conditions through Pt that essentially promoted the multielectron reduction reaction on O₂ to produce superoxide and hydroxyl radicals to degrade HCHO into CO₂ under dark conditions.

As discussed in earlier cases, the oxidative energy-storage ability of the $\text{TiO}_2/\text{Ni}(\text{OH})_2$ PC was evaluated for the degradation of monocarbon compounds, such as methanol and formaldehyde into CO_2 under dark conditions. Recently, this system was also found to degrade multicarbon compounds, such as acetaldehyde, acetic acid, and acetone, into CO_2 in the dark.^[44] Additionally, it was proposed that MnO_x could also be used as an oxidative energy-storage material; however, the direct integration of MnO_x with TiO_2 was not feasible, but could be achieved by introducing an interface material, such as fluorine-doped tin oxide (FTO)/ MnO_x /nanoporous $\text{SiO}_2/\text{TiO}_2$. This feature was explained as follows: direct contact of MnO_x with TiO_2 leads to greater reduction reaction, rather than oxidation reaction to store the oxidative energy. Interestingly, the separation of MnO_x and TiO_2 by SiO_2 , with an optimum thickness, induces the oxidation of the MnO_x layer, as depicted in Figure 11. If

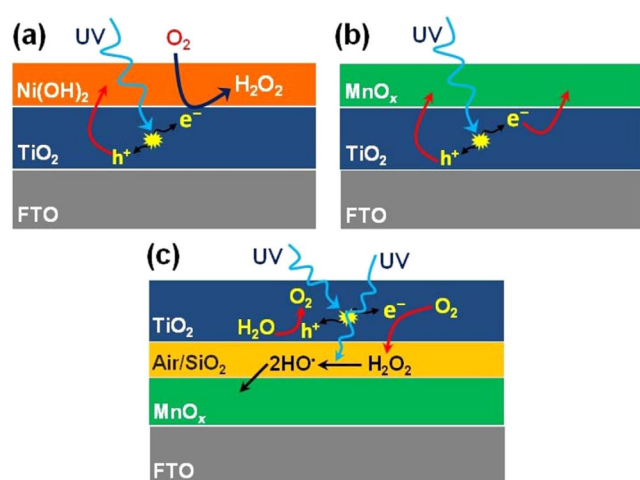
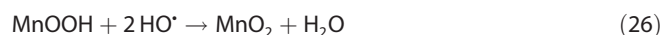
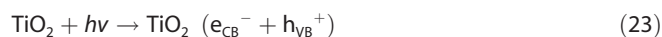
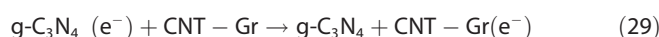
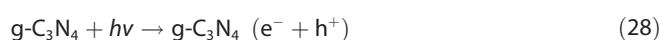


Figure 11. Oxidative energy-storage behavior in a) $\text{TiO}_2/\text{Ni}(\text{OH})_2$, b) $\text{TiO}_2/\text{MnO}_x$, and c) $\text{FTO}/\text{MnO}_x/\text{air}$ (or nanoporous SiO_2)/ TiO_2 systems under UV-light irradiation.

TiO_2 is excited, the electrons in CB react with O_2 and H^+ species and produce H_2O_2 , which further dissociates into hydroxyl radicals under UV light and oxidizes MnO_x , as shown in Equations (23)–(26). In an alternative mechanism, the hydroxyl radicals may be produced through the direct photocatalytic oxidation of H_2O by TiO_2 [Eq. (27)]. Accordingly, the successfully developed photocharged $\text{FTO}/\text{MnO}_x/\text{nanoporous } \text{SiO}_2/\text{TiO}_2$ system was found to mineralize methanol, acetaldehyde, acetic acid, and acetone under dark conditions.



Another unconventional and metal-free carbon-based material, which is a nanocomposite composed of $g\text{-C}_3\text{N}_4\text{-CNTs-Gr}$, was developed to have a postillumination catalytic memory effect and investigated for the removal of phenol under dark conditions.^[47] It was reported that $g\text{-C}_3\text{N}_4$ acted an efficient PC, whereas CNTs and Gr acted as supercapacitors to store and discharge the charges under illumination and dark conditions, respectively. Based on a radical trapping experiment, the mechanism of the observed day–night photocatalytic effect of $g\text{-C}_3\text{N}_4\text{-CNTs-Gr}$ was proposed as follows: during light irradiation, electrons excited to the CB of $g\text{-C}_3\text{N}_4$ are further transferred to the surface and bulk of CNT–Gr. Electrons transferred to the surface react with O_2 to produce superoxide radicals and degrade phenol under visible light [Eqs. (28)–(30)], whereas electrons in the bulk, which are trapped, react with $\text{O}_2/\text{H}_2\text{O}$ to produce $\cdot\text{OH}$ radicals [Eq. (31)] and effectively degrade phenol under dark conditions.



4.2. Hydrogen productions

$g\text{-C}_3\text{N}_4$ modified with cyanamide-functionalized heptazine polymer was demonstrated to be a prospective material for the generation of hydrogen in the dark.^[48] It was proposed that, during the irradiation of $g\text{-C}_3\text{N}_4$, radical species formed within a cyanamide-functionalized polymeric network of heptazine units could release trapped electrons in the dark to produce H_2 . It was reported from experiments carried out that $g\text{-C}_3\text{N}_4$ consisted of a partially anionic and cyanamide-functionalized heptazine, along with an appropriate electron donor, which led to the formation a radical species under light irradiation with a lifetime of over 10 h. This ultra-long-lived radical can reductively produce H_2 under dark conditions in the presence of a hydrogen evolution catalyst. Furthermore, it was described that the continuous photocharging and storing effect of the reported modified $g\text{-C}_3\text{N}_4$ compound could be perform a capacitor-like function of the photocatalyst with the potential to become “solar battery” materials.

4.3. Bactericidal disinfections

$\text{TiO}_2\text{-WO}_3$ was also found to be a prototypical system for photocatalytic antibactericidal applications in the dark.^[28] The exploration of $\text{TiO}_2\text{-WO}_3$ for such antibacterial applications essentially helped to understand the possible mechanism of their photocatalytic activity in the dark. Accordingly, $\text{TiO}_2\text{-WO}_3$ was successfully employed for antibacterial activity against *E. coli* bacteria under dark conditions. From the experimental studies conducted, the origin of the observed antibacterial activity of the system was mainly due to the generation of H_2O_2 species produced upon the reaction between stored electrons and O_2 molecules in the dark.

A nanocomposite of TiON/PdO was studied for the photocatalytic disinfection of *E. coli* in the dark.^[32,66] It was observed that PdO was the origin of the observed electron storage and dark antibacterial properties of the nanocomposite. The antibacterial effect was found to persist even after several hours in the dark. It was proposed that electron storage occurred in TiON/PdO system essentially due to the transfer of electrons from TiON to PdO, for which PdO is reduced to Pd⁰ and traps electrons in Pd⁰ nanoparticles. In the dark, these stored electrons are released back to the environment to react with O₂ and produce O₂⁻/ \cdot OH radicals to kill the bacteria, as shown in Figure 12. A similar mechanism, which is the stored electron-mediated production of redox species, was also reported for the antibacterial activity in the TiO₂/Cu₂O system towards *E. coli*,^[41] SnO₂ nanoparticles decorated Cu₂O nanocubes towards *Staphylococcus aureus*,^[45] titanium oxide system^[67] towards *Enterococcus faecalis*, and *E. coli* under dark conditions (Figure 10a and b).

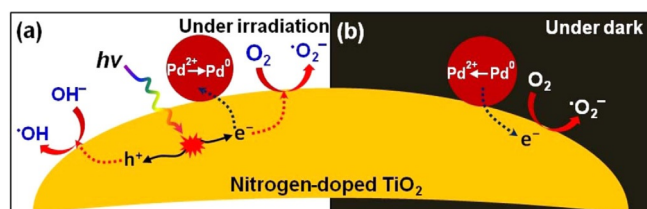


Figure 12. Reduction-mediated electron storage and release in the TiON/PdO system towards antibacterial activity under light irradiation (a) and dark (b) conditions.

4.4. Heavy-metal reductions

The photoinduced electron-storage properties of the WO₃/TiO₂ system were also explored for its application in the reduction of heavy-metal ions, such as Cr⁶⁺, Hg²⁺, and Ag⁺, into their corresponding, relatively nontoxic, and stable states, such as Cr³⁺, Hg⁺, and Ag⁰, respectively.^[68] This study essentially showed that stored electrons were capable of reducing heavy-metal ions in the dark as well. WO₃/TiO₂ is charged under UV-light irradiation and stores electrons for a longer time in the presence of O₂, and can be discharged through a suitable reduction process. In practice, the presence of O₂ inhibits the storage of electrons by scavenging them. However, electron scavenging by O₂ produces the reactive species, such as O₂⁻ and H₂O₂, required for the degradation/reduction process. Therefore, O₂ is useful to scavenge electrons released in the dark to produce reductive species; meanwhile, a parallel mechanism should also be needed to inhibit the scavenging of electrons during light irradiation. Accordingly, it was experimentally observed that the capture rate of electrons by WO₃ was much faster than that of O₂. Through this mechanism, electrons excited to the CB of TiO₂ are further transferred to WO₃ to form W⁵⁺ ions; protons are subsequently expected to intercalate into WO₃/TiO₂ to balance the charge neutrality of the system as a result of negative charge induced by the stored electrons. During the dark reaction, the reduction of O₂ by

stored electrons in the form of W⁵⁺ was much higher (almost fivefold) than that of the stored electrons in the form of Ti³⁺. Therefore, the integration of WO₃ simultaneously enhanced electron storage and the reduction of O₂ to produce reductive species to reduce the heavy-metal ions. In addition, the spontaneous reduction of Cr^{VI} was also observed on InSnS₂ PC under dark conditions.^[69]

Similarly, a recent study showed an interesting feature of this day–night photocatalytic system, which was sequential catalytic activity under light and dark conditions. In a single reaction, organic pollutants, such as 4-CP, formic acid, humic acid, or ethanol, were degraded with Ag/TiO₂ under UV light, followed by the dark reduction of hexavalent Cr^{VI}.^[70] It was reported that the photocatalytic oxidation of 4-CP produced intermediate compounds and stored electrons in the Ag/TiO₂ system for further utilization to reduce Cr^{VI} in the dark. Accordingly, the dark reduction of Cr^{VI} was much higher for Ag/TiO₂ (87%) and continued for few hours. The observed dark-reduction efficiency of the Ag/TiO₂ system was proposed to be the collective effects of 1) adsorption, 2) chemical reduction by intermediates of 4-CP degradation, and 3) reduction by electrons stored in Ag (Figure 13).

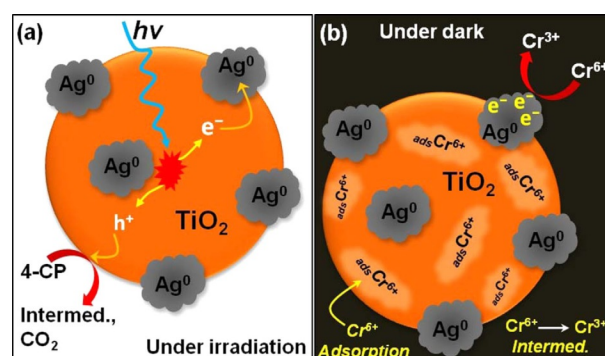


Figure 13. a) Photocatalytic electron storage and degradation under illumination, and b) sequential reduction of metals (Cr⁶⁺ to Cr³⁺) in the dark by Ag–TiO₂ PC.

4.5. Other applications

As discussed, the classical application of an electron-storage system was essentially for the anticorrosion of metals, for which the ESM was first developed. It was reported that the corrosion properties of TiO₂-coated type-304 stainless steel were suppressed under UV irradiation;^[71] however, to protect the material, even in the dark, ESMs such as WO₃^[22,72] or SnO₂^[73] were coated along with TiO₂ onto the metal. Based on insights from these studies,^[22] the characteristics of the ESM towards anticorrosion properties were suggested to be as follows: 1) redox activity; 2) a more positive redox potential than that of the CB potential of the semiconductor attached, that is, the oxidized form of the ESM should accept electrons from the semiconductor; 3) a more negative redox potential than that of the corrosion potential of the metal, that is, the reduced form should protect the metal from corrosion; 4) poor oxidizability of the reduced form by ambient oxygen; and 5) stability

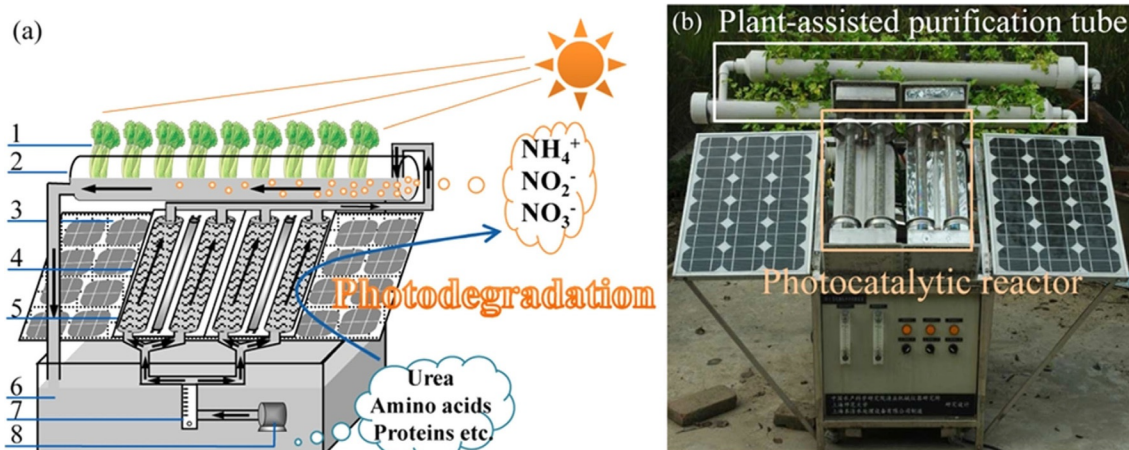
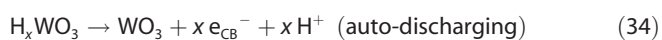
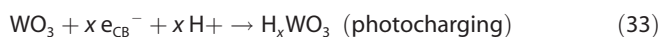


Figure 14. a) Schematic diagram and b) photograph of the plant-assisted photocatalytic reactor: 1) celery, 2) plant cultivation tube, 3) solar battery, 4) quartz glass tube coated with the $\text{Bi}_2\text{O}_3/\text{TiO}_2$ film PC, 5) UV lamp, 6) water reservoir, 7) liquid flow meter, and 8) circulation pump.

during repeated redox cycles. Accordingly, the photocharging and discharging reactions in the $\text{TiO}_2\text{--WO}_3$ system are described by Equations (32)–(34). Briefly, the $\text{TiO}_2\text{--WO}_3$ system provides photoelectrons to the metal through a cascading potential of $\text{TiO}_2\text{--WO}_3\text{--metal}$ (during irradiation) and $\text{WO}_3\text{--metal}$ (during dark).^[72]



An interesting application has been demonstrated to represent round-the-clock photocatalysis.^[74] The system for this particular application involved a photocatalytic reactor equipped with solar batteries, $\text{Bi}_2\text{O}_3/\text{TiO}_2$ PC, and celery plant towards the purification of aquaculture wastewater under solar-light irradiation (Figure 14). Solar batteries in the system convert sunlight into stored electrical energy to power UV lamps, which further lead to round-the-clock photocatalytic degradation of organonitrogen pollutants. Meanwhile, the degraded organonitrogen pollutants (into inorganic nitrogen species) will be taken up by the plant as a fertilizer, which eventually leads to the complete purification of the aquaculture wastewater.

Apart from application-oriented studies, conventional systems, such as $\text{TiO}_2\text{--WO}_3$,^[75–80] and $\text{TiO}_2\text{--Ni(OH)}_2$,^[81–85] have been exclusively studied for their photocharging and discharging mechanisms, which could be potentially useful for the development of day–night-based photocatalytic systems. It is known that photocatalysis is being widely employed for pollutant degradation, water splitting, and fuel conversion applications. However, there are other interesting applications of photocatalysis, including 1) medicinal applications, such as cancer treatments,^[86,87] bioimplants,^[88,89] and removal of airborne biological threats (e.g., Anthrax);^[90,91] 2) agricultural applications;^[92] 3) atmospheric sciences;^[93] 4) biodiesel productions;^[94] and 5) organic syntheses,^[95] which are untapped potential applications in the field of photocatalytic sciences that should be

explored, along with the utilization of ESMs towards day–night photocatalytic applications.

5. Summary and Outlook

It is undoubtedly true that photocatalytic science is remarkable for its applications in energy and environmental concerns. Therefore, it is imperative to find more tools to enhance the features and functions of photocatalytic materials to transcend existing limitations in the photocatalysis process. In this context, the integration of an ESM with a PC to catalyze a reaction in the presence and absence of light can be essentially considered as the next promising step in this field. Such advancement should be accelerated further because it has the potential to be a next-generation photocatalytic technique. Insights derived from these studies clearly highlight that the ESMs are often narrow band gap energy materials that facilitate charge separation and transportation, which are the most fundamental characteristics required for an efficient photocatalytic process. Apart from electron storage and release, these additional features of ESMs “synergistically sensitize” a PC towards its ideal function. Based on the proposed mechanisms, materials with intercalation and/or reducing properties with suitable band edge positions, with respect to the host PC, could be appropriate for the construction of a day–night photocatalytic system. ESMs should be enhanced for their electron-storage ability, longevity, rapid charging, gradual discharging, photochemical stability, and durability by means of chemical and physical modifications.

Future scope in the utilization of ESMs should be explored for various applications of photocatalytic processes, as mentioned above. Also, similar tools have to be built according to the specific needs of the photocatalytic applications/processes. This multifaceted photocatalytic phenomenon is promisingly for new possibilities in the fields of healthcare, environment, and energy applications because these are the three fundamental requirements for life on this planet.

Acknowledgements

This work was supported by the Natural Science and Engineering Research Council of Canada (NSERC) through the Collaborative Research and Development (CRD), Strategic Project (SP), and Discovery Grants (DG). We would also like to thank EXP Inc. and SiliCycle Inc. for their support.

Conflict of interest

The authors declare no conflict of interest.

Keywords: electron-storage materials · intercalations · materials science · photocatalysis · redox chemistry

- [1] L. Mohapatra, K. Parida, *Catal. Sci. Technol.* **2017**, *7*, 2153–2164.
- [2] X. Hu, G. Li, J. C. Yu, *Langmuir* **2010**, *26*, 3031–3039.
- [3] D. Li, W. Shi, *Chin. J. Catal.* **2016**, *37*, 792–799.
- [4] S. R. Lingampalli, M. M. Ayyub, C. N. R. Rao, *ACS Omega* **2017**, *2*, 2740–2748.
- [5] T. Hisatomi, J. Kubota, K. Domen, *Chem. Soc. Rev.* **2014**, *43*, 7520–7535.
- [6] H. Tong, S. Ouyang, Y. Bi, N. Umezawa, M. Oshikiri, J. Ye, *Adv. Mater.* **2012**, *24*, 229–251.
- [7] W. Tu, Y. Zhou, Z. Zou, *Adv. Funct. Mater.* **2013**, *23*, 4996–5008.
- [8] P. V. Kamat, *ACS Energy Lett.* **2017**, *2*, 1586–1587.
- [9] A. L. Linsebigler, G. Lu, J. T. Yates, *Chem. Rev.* **1995**, *95*, 735–758.
- [10] J. Schneider, M. Matsuoka, M. Takeuchi, J. Zhang, Y. Horiuchi, M. Anpo, D. W. Bahnemann, *Chem. Rev.* **2014**, *114*, 9919–9986.
- [11] Y. Navarro Yerga, M. Rufino, G. Alvarez, M. Consuelo, F. del Valle, M. Villoriadela, A. Jose, J. L. G. Fierro, *ChemSusChem* **2009**, *2*, 471–485.
- [12] J. Xing, W. Q. Fang, H. J. Zhao, H. G. Yang, *Chem. Asian J.* **2012**, *7*, 642–657.
- [13] a) X. Wang, F. Wang, Y. Sang, H. Liu, *Adv. Energy Mater.* **2017**, *7*, 1700473; b) Y. Sang, H. Liu, A. Umar, *ChemCatChem* **2015**, *7*, 559–573.
- [14] A. Kubacka, M. Fernández-García, G. Colón, *Chem. Rev.* **2012**, *112*, 1555–1614.
- [15] D. Zhang, G. Li, H. Li, Y. Lu, *Chem. Asian J.* **2013**, *8*, 26–40.
- [16] A. Kudo, *Int. J. Hydrogen Energy* **2007**, *32*, 2673–2678.
- [17] X. Wu, S. Yin, Q. Dong, B. Liu, Y. Wang, T. Sekino, S. W. Lee, T. Sato, *Sci. Rep.* **2013**, *3*, 2918.
- [18] X. Li, J. Yu, M. Jaroniec, *Chem. Soc. Rev.* **2016**, *45*, 2603–2636.
- [19] H. Yan, X. Wang, M. Yao, X. Yao, *Prog. Nat. Sci.* **2013**, *23*, 402–407.
- [20] a) X. Hu, Y. Li, J. Tian, H. Yang, H. Cui, *J. Ind. Eng. Chem.* **2017**, *45*, 189–196; b) S. Ganguli, C. Hazra, M. Chatti, T. Samanta, V. Mahalingam, *Langmuir* **2016**, *32*, 247–253.
- [21] T. Tatsuma, S. Saitoh, Y. Ohko, A. Fujishima, *Chem. Mater.* **2001**, *13*, 2838–2842.
- [22] T. Tatsuma, S. Saitoh, P. Ngaotrananwivat, Y. Ohko, A. Fujishima, *Langmuir* **2002**, *18*, 7777–7779.
- [23] P. G. Dickens, M. S. Q. Whittingham, *Rev. Chem. Soc.* **1968**, *22*, 30–44.
- [24] Y. Takahashi, T. Tatsuma, *Langmuir* **2005**, *21*, 12357–12361.
- [25] L. Xiong, M. Ouyang, L. Yan, J. Li, M. Qiu, Y. Yu, *Chem. Lett.* **2009**, *38*, 1154–1155.
- [26] J. P. Yasomane, J. Bandara, *Sol. Energy Mater. Sol. Cells* **2008**, *92*, 348–352.
- [27] G. Li, Y. Zhang, L. Wu, F. Wu, R. Wang, D. Zhang, J. Zhu, H. Li, *RSC Adv.* **2012**, *2*, 4822–4828.
- [28] T. Tatsuma, S. Takeda, S. Saitoh, Y. Ohko, A. Fujishima, *Electrochem. Commun.* **2003**, *5*, 793–796.
- [29] P. Ngaotrananwivat, T. Tatsuma, *J. Electroanal. Chem.* **2004**, *573*, 263–269.
- [30] Y. Takahashi, P. Ngaotrananwivat, T. Tatsumav, *Electrochim. Acta* **2004**, *49*, 2025–2029.
- [31] Y. Takahashi, T. Tatsuma, *Electrochem. Commun.* **2008**, *10*, 1404–1407.
- [32] Q. Li, W. Li, P. Wu, R. Xie, J. K. Shang, *Adv. Mater.* **2008**, *20*, 3717–3723.
- [33] C.-T. Wang, H.-H. Huang, *J. Non-Cryst. Solids* **2008**, *354*, 3336–3342.
- [34] H. Huang, L. Jiang, W. K. Zhang, Y. P. Gan, X. Y. Tao, H. F. Chen, *Sol. Energy Mater. Sol. Cells* **2010**, *94*, 355–359.
- [35] C. Ng, Y. H. Ng, A. Iwase, R. Amal, *Phys. Chem. Chem. Phys.* **2011**, *13*, 13421–13426.
- [36] A. Kongkanand, P. V. Kamat, *ACS Nano* **2007**, *1*, 13–21.
- [37] A. Takai, P. V. Kamat, *ACS Nano* **2011**, *5*, 7369–7376.
- [38] F. Yang, Y. Takahashi, N. Sakai, T. Tatsuma, *J. Phys. Chem. C* **2011**, *115*, 18270–18274.
- [39] F. Yang, Y. Takahashi, N. Sakai, T. Tatsuma, *J. Mater. Chem.* **2011**, *21*, 2288–2293.
- [40] J. Li, Y. Liu, Z. Zhu, G. Zhang, T. Zou, Z. Zou, S. Zhang, D. Zeng, C. Xie, *Sci. Rep.* **2013**, *3*, 2409.
- [41] L. Liu, W. Yang, Q. Li, S. Gao, J. K. Shang, *ACS Appl. Mater. Interfaces* **2014**, *6*, 5629–5639.
- [42] A. Molla, M. Sahu, S. Hussain, *J. Mater. Chem. A* **2015**, *3*, 15616–15625.
- [43] C. C. Nguyen, N. N. Vu, T. O. Do, *J. Mater. Chem. A* **2016**, *4*, 4413–4419.
- [44] Y. Kuroiwa, S. Park, N. Sakaia, T. Tatsuma, *Phys. Chem. Chem. Phys.* **2016**, *18*, 31441–31445.
- [45] L. Liu, W. Sun, W. Yang, Q. Li, J. K. Shang, *Sci. Rep.* **2016**, *6*, 20878.
- [46] S. Buama, P. Ngaotrananwivat, P. Rangsanvigit, *Chem. Eng. J.* **2017**, *309*, 866–872.
- [47] Q. Zhang, H. Wang, Z. Li, C. Geng, J. Leng, *ACS Appl. Mater. Interfaces* **2017**, *9*, 21738–21746.
- [48] V.-W. Lau, D. Klose, H. Kasap, F. Podjaski, M.-C. Pignié, E. Reisner, G. Jeschke, B. V. Lotsch, *Angew. Chem. Int. Ed.* **2017**, *56*, 510–514; *Angew. Chem.* **2017**, *129*, 525–529.
- [49] G. R. S. Andrade, C. C. Nascimento, E. C. Silva Júnior, D. T. S. L. Mendes, I. F. Gimenez, *J. Alloys Compd.* **2017**, *710*, 557–566.
- [50] W. H. Saputera, J. A. Scott, D. Friedmann, R. Amal, *Appl. Catal. B: Environ.* **2018**, *223*, 216–227.
- [51] J. Gupta, J. Mohapatra, D. Bahadur, *Dalton Trans.* **2017**, *46*, 685–696.
- [52] Y. H. Lin, C. H. Weng, J. H. Tzeng, Y. T. Lin, *Int. J. Photoenergy* **2016**, *2016*, 3058429.
- [53] Y. Zhang, Q. Li, C. Liu, X. Shan, X. Chen, W. Dai, X. Fu, *Appl. Catal. B* **2018**, *224*, 283–294.
- [54] A. Molla, M. Sahu, S. Hussain, *Sci. Rep.* **2016**, *6*, 26034.
- [55] J. Gamage McEvoy, Z. Zhang, *J. Photochem. Photobiol. C* **2014**, *19*, 62–75.
- [56] P. V. Lakshmi, V. Rajagopalan, *Sci. Rep.* **2016**, *6*, 38606.
- [57] X. Zhang, X. Li, D. Zhang, N. Q. Su, W. Yang, H. O. Everitt, J. Liu, *Nat. Commun.* **2017**, *8*, 14542.
- [58] H. Yin, X. Chen, R. Hou, H. Zhu, S. Li, Y. Huo, H. X. Li, *ACS Appl. Mater. Interfaces* **2015**, *7*, 20076–20082.
- [59] F. Li, Z. Li, Y. Cai, M. Zhang, Y. Shen, W. Wang, *Mater. Lett.* **2017**, *208*, 111–114.
- [60] Y. Lu, X. Zhang, Y. Chu, H. Yu, M. Huo, J. Qua, J. C. Crittenden, H. Huo, X. Yuan, *Appl. Catal. B* **2018**, *224*, 239–248.
- [61] Q. Zhou, F. Peng, Y. Ni, J. Kou, C. Lu, Z. Xu, *J. Photochem. Photobiol. A* **2016**, *328*, 182–188.
- [62] I. P. Sahu, D. P. Bisen, N. Brahma, R. Sharma, *Res. Chem. Intermed.* **2015**, *41*, 6649–6664.
- [63] W. Pan, G. Ning, X. Zhang, J. Wang, Y. Lin, J. Ye, *J. Lumin.* **2008**, *128*, 1975–1979.
- [64] a) F. Yang, Y. Takahashi, N. Sakai, T. Tatsuma, *Phys. Chem. Chem. Phys.* **2010**, *12*, 5166–5170; b) Y. Takahashi, T. Tatsuma, *Phys. Chem. Chem. Phys.* **2006**, *8*, 2716–2719.
- [65] Y. Li, L. Chen, Y. Guo, X. Sun, Y. Wei, *Chem. Eng. J.* **2012**, *181–182*, 734–739.
- [66] Q. Li, Y. W. Li, Z. Liu, R. Xie, J. K. Shang, *J. Mater. Chem.* **2010**, *20*, 1068–1072.
- [67] G. Wang, Z. Xing, X. Zeng, C. Feng, D. T. McCarthy, A. Deletic, X. Zhang, *Nanoscale* **2016**, *8*, 18050–18056.
- [68] D. Zhao, C. Chen, C. Yu, W. Ma, J. Zhao, *J. Phys. Chem. C* **2009**, *113*, 13160–13165.
- [69] S. Park, W. Kim, R. Selvaraj, Y. Kim, *Chem. Eng. J.* **2017**, *321*, 97–104.
- [70] Y. Choi, M. S. Koo, A. D. Bokare, D.-H. Kim, D. W. Bahnemann, W. Choi, *Environ. Sci. Technol.* **2017**, *51*, 3973–3981.
- [71] Y. Ohko, S. Saitoh, T. Tatsuma, A. Fujishima, *J. Electrochem. Soc.* **2001**, *148*, B24–B28.
- [72] H. Park, A. Bak, T. H. Jeon, S. Kim, W. Choi, *Appl. Catal. B* **2012**, *115–116*, 74–80.

- [73] R. Subasri, T. Shinohara, *Electrochem. Commun.* **2003**, *5*, 897–902.
- [74] Z. Bian, F. Cao, J. Zhu, H. Li, *Environ. Sci. Technol.* **2015**, *49*, 2418–2424.
- [75] P. Ngaotranakawiat, T. Tatsuma, S. Saitoh, Y. Ohko, A. Fujishima, *Phys. Chem. Chem. Phys.* **2003**, *5*, 3234–3237.
- [76] L. Cao, J. Yuan, M. Chen, W. Shangguan, *J. Environ. Sci.* **2010**, *22*, 454–459.
- [77] Y. Liu, C. Xie, H. Li, H. Chen, T. Zou, D. Zeng, *J. Hazard. Mater.* **2011**, *196*, 52–58.
- [78] D. Liu, W. Zi, S. D. Sajjad, C. Hsu, Y. Shen, M. Wei, F. Liu, *ACS Catal.* **2015**, *5*, 2632–2639.
- [79] W. K. Zhang, L. Wang, H. Huang, Y. P. Gan, C. T. Wang, X. Y. Tao, *Electrochim. Acta* **2009**, *54*, 4760–4763.
- [80] L. Zhang, L. Xu, J. Wang, H. Shao, Y. Fan, J. Zhang, *J. Phys. Chem. C* **2011**, *115*, 18027–18034.
- [81] H. Q. Lian, J. M. Wang, L. Xu, L. Y. Zhang, H. B. Shao, J. Q. Zhang, C. N. Cao, *Electrochim. Acta* **2011**, *56*, 2074–2080.
- [82] L. Zhang, L. Xu, J. Wang, J. Cai, J. Xu, H. Zhou, Y. Zhong, D. Chen, J. Zhang, C. Cao, *J. Electroanal. Chem.* **2012**, *683*, 55–61.
- [83] Y. Takahashi, T. Tatsuma, *Electrochemistry* **2014**, *82*, 749–751.
- [84] J. Gamage, Z. Zhang, *Int. J. Photoenergy* **2010**, 764870.
- [85] A. Fujishima, T. N. Rao, D. A. Tryk, *J. Photochem. Photobiol. C* **2000**, *1*, 1–21.
- [86] Y. Kubota, T. Shuin, C. Kawasaki, M. Hosaka, H. Kitamura, R. Cai, H. Sakai, K. Hashimoto, A. Fujishima, *Br. J. Cancer* **1994**, *70*, 1107–1111.
- [87] O. L. Kaliya, E. A. Lukyanets, G. N. Vorozhtsov, *J. Porphyrins Phthalocyanines* **1999**, *3*, 592–610.
- [88] C. Lee, H. Choi, C. Lee, H. Kim, *Surf. Coat. Technol.* **2003**, *173*, 192–200.
- [89] P. Evans, D. W. Sheel, *Surf. Coat. Technol.* **2007**, *201*, 9319–9324.
- [90] J. H. Kau, D. S. Sun, H. H. Huang, M. S. Wong, H. C. Lin, H. H. Chang, *PLoS ONE* **2009**, *4*, e4167.
- [91] S. H. Lee, S. Pumprueg, B. Moudgil, W. Sigmund, *Colloids Surf. B* **2005**, *40*, 93–98.
- [92] Y. Wang, C. Sun, X. Zhao, B. Cui, Z. Zeng, A. Wang, G. Liu, H. Cui, *Nano-scale Res. Lett.* **2016**, *11*, 529.
- [93] H. Chen, C. E. Nanayakkara, V. H. Grassian, *Chem. Rev.* **2012**, *112*, 5919–5948.
- [94] G. Corro, U. Pal, N. Tellez, *Appl. Catal. B* **2013**, *129*, 39–47.
- [95] D. Friedmann, A. Hakki, H. Kim, W. Choi, D. W. Bahnemann, *Green Chem.* **2016**, *18*, 5391–5411.

Manuscript received: November 26, 2017

Revised manuscript received: December 21, 2017

Accepted manuscript online: January 8, 2018

Version of record online: February 19, 2018